JOURNAL OF PROPULSION AND POWER
Vol. 24, No. 5, September–October 2008

Multiple Objective Optimization and Inverse Design of Axial Turbomachinery Blades

Francesco Larocca*
Politecnico di Torino, I-10129 Turin, Italy

DOI: 10.2514/1.33894

An optimization procedure, based on a method for solving inverse problems for the design of whole multistage axial turbines and compressors, is presented in the paper. A simplified axisymmetric model of three-dimensional axial turbomachines is adopted in which volume forces replace the stator and rotor. The tangential component of such blade forces represents the design parameters that are defined through the optimization algorithm, whereas the stream surfaces that represent the stators and rotors are obtained by solving the inverse flow problem governed by the time-dependent Euler equations. The current optimization procedure takes into account some three-dimensional effects, such as lean and sweep, in the early stages of the design of blade rows by directly controlling the blade loading. The optimization process is based on a multi-objective genetic algorithm in which a search for an optimal Pareto front is performed. Some preliminary numerical examples, which refer to the design of a linear cascade and compressor stage, are discussed.

Nomenclature

B	=	projection on the meridional plane of the blade
b, d, h	=	blockage factor, cascade pitch, and free passage
E, H	=	total energy per unit mass, total enthalpy per unit mass
F, G	=	flux vectors
$\mathbf{F}_b$	=	blade force per unit volume
$\mathbf{F}_f$	=	friction force per unit volume
N, Q	=	source term vectors
$\mathbf{n}$	=	normal unit vector
p, T	=	pressure, temperature
$\mathbf{q}$	=	velocity vector
$\mathbf{r}$	=	radius vector
s	=	entropy per unit mass
t	=	time
U	=	conservative variable vector
u, v, w	=	axial, tangential, and radial components of the flow velocity
x, θ, r	=	axial, tangential, and radial coordinates
δ	=	tangential blade thickness
ρ	=	density
σ, τ	=	surface and volume elements of D
$\mathbf{\Omega}$	=	angular velocity vector

Subscripts

r, x, θ	=	radial, axial, and tangential vector components

Superscript

0	=	total quantities

I. Introduction

THE increasing demands for enhanced performances of jet engines have driven efforts toward a better description and prediction of complex flow phenomena through axial turbomachines. Computational fluid dynamics (CFD) plays a key role in the design of the whole engine; sophisticated numerical tools that are capable of simulating the inherently unsteady, viscous, three-dimensional flow through multiple blade rows quite accurately and that allow more efficient engines to be defined in less time have been developed. However, great efforts are still required by the designer to find better solutions, and the development of an innovative aerodynamic configuration is a challenging problem, especially considering the time needed to establish a new optimal design. This is mainly due to the fact that the design process, in normal industrial practice, has a sequential nature and is primarily based on a trial and error procedure: one starts from an initial configuration for which the main design choices are made and then proceeds with subsequent refinements using more and more sophisticated CFD analysis tools to obtain a satisfactory flow configuration. Three-dimensional simulations tend to be used in the early design process to reduce the cycles in the design process; however, even with the increasing capability of computing resources, the computational times required for 3-D analysis still represent a drawback in the search for optimized configurations. The high computational costs of 3-D solvers make direct numerical optimization extremely expensive, and this makes it impracticable for the design of a new project within an acceptable time frame. Inverse methods based on CFD techniques for three-dimensional turbomachinery blading design, which allow the profile of the blades to be produced to satisfy assigned properties of the flowfield, can considerably reduce the cycles in the iterative procedure, but they are used in the design of the individual components and, if coupled with an optimization algorithm, they can offer the same limitations as direct methods, because the three-dimensional computational costs are still high. A design system based on a parametric representation, advanced CFD, and numerical optimization algorithms could be a very promising tool for the design of a multicomponent turbomachine [1].

Simplified flow solvers, such as a throughflow model, are, however, still necessary as an essential tool to obtain an optimized design of multistage turbines and compressors [2]. Classical streamline curvature/stream function methods of throughflow models for the design of turbomachines tend to be replaced by the time-marching techniques that solve the Euler [3] and, more recently, the Navier–Stokes [4] equations in the meridional plane. By bringing more physics into the model, they can overcome some limits of the streamline curvature methods and they offer the advantage, among others, of allowing the introduction of some 3-D blade features, such as lean and sweep effects, into the throughflow design.

A method for an efficient and simple axisymmetric phase of the design process, which is capable of providing the camber surfaces of

Received 6 August 2007; revision received 19 May 2008; accepted for publication 20 May 2008.

*Associate Professor, Dipartimento Ingegneria Aeronautica e Spaziale, Corso Duca degli Abruzzi, 24; francesco.larocca@polito.it.

the blades of an entire axial machine [5], has been adopted in this paper. The flow deflection through the rotors and stators is the result of the angular momentum change due to the forces that the blades exert on the flow. An axisymmetric model of a 3-D turbomachine can be set up by replacing the blade rows with volume forces wherein, assuming the flow is inviscid, a single blade row coincides with a stream surface orthogonal to the forces themselves. An inverse problem is then formulated by prescribing the tangential component of such volume forces along the radial and axial directions as the design data and by searching for blade camber surfaces. The rotors and stators are considered the stream surfaces of the relative and absolute motion, respectively, and their geometries are determined according to a finite volume time-marching integration of the Euler equations in the meridional plane. The method is therefore different from the throughflow design model proposed in [3], in which the unsteady axisymmetric Euler equations are solved in the meridional plane and the swirl velocity along the span at the trailing edge of each blade row is specified as the design data.

The process used to obtain the numerical solution is the one described in [6,7], in which the inverse technique is used to design two-dimensional/axisymmetric nozzles and intakes by prescribing pressure distribution along the walls, and in [8], in which the inverse problem is solved to evaluate the geometry of three-dimensional blade rows when blade loading and blade thickness are specified as the design data along the axial and radial directions. A similar approach to the inverse problems for the design of 3-D blade rows has been developed independently in [9].

The main weakness related to the inverse design is due to the difficulty of specifying the proper design data (e.g., the blade loading), because they do not have a direct correspondence with the blade geometry; much is left to the experience of the designer and his/her ability to define a suitable distribution of the loading and, as such, a high degree of arbitrariness may be introduced. To overcome these drawbacks and the inability to minimize/maximize global quantities, the inverse problem can be inserted into an optimization algorithm.

Among the optimization techniques, evolutionary strategies are increasingly and successfully being adopted for a wide variety of problems in mechanical and aerodynamic design. Interest in the use of stochastic techniques as a genetic algorithm (GA) depends on their simplicity and robustness, their ability to overcome some weaknesses of classical gradient-based optimizations, their capability of handling a large number of design variables. and, finally, on the need for an efficient approach to multidisciplinary and multi-objective design problems [10–12]. The large amount of computational time required for the simulations, when a high number of geometrical/physical design parameters is involved, is the main drawback of GAs. Parallel computing, efficient parameterization, knowledge-based GAs, hybrid optimization algorithms, and simplified physics, or surrogate models, all represent valid artifices that make these methods attractive for solving complex search and optimization problems [13–15].

In this work, the proposed design method of the axisymmetric model of the turbomachine has been inserted into a multi-objective GA. As opposed to the shape optimization, in which the design variables are geometrical quantities, in the present inverse optimization, the control is given by the blade loading and constraints can act directly on it. In the optimization process, the functional that has to be maximized/minimized is evaluated by solving the time-dependent Euler equations on the meridional plane, whereas the parameters that describe the distribution of the tangential component of the blade forces are assumed as design variables. The blade camber is obtained from the solution of the inverse problem, whereas the blade loading itself is modified according to the objectives that have to be pursued. Moreover, the search space can be defined and amplified by considering a wide set of other design variables (e.g., the stacking line, sweep and lean of the blades, and chord length). On the other hand, it can also be confined by equality and inequality constraints (e.g., the work per stage and work distribution, flow angle, and geometrical/mechanical requirements).

In the current optimization procedure, interest is focused on the appealing possibilities of becoming aware of some three-dimensional effects in the early stage of the design of blade rows of a turbomachine via a direct control of the loading and, as a consequence, the work. In the following sections, the affordability of the approach is investigated by searching for optimized blade loading distribution and blade lean and sweep, which minimize suitable cost functions. In the design examples reported herein, the purely inviscid Euler equations are solved without models that account for end walls or profile losses. Therefore, the functional merit does not take into account the overall performance as was done, for example, in [16], in which a throughflow method, based on a stream function method with loss models, is used on a hybrid constrained optimization process to optimize hub and shroud geometries and tangential velocity components at each blade exit row that provide a maximum efficiency for a multistage turbine.

In the next sections, an outline of the inverse method, the numerical implementation, and some key elements of the GA are first presented. Some three-dimensional aspects are then discussed and, finally, the results that refer to the design of a linear cascade and a single compressor stage are illustrated.

II. Throughflow Model

This model is based on the unsteady Euler equations written on the meridional plane. The action of blade rows is accounted for by introducing a volume force, $\mathbf{F}_b$, which is responsible for flow turning and is orthogonal to the stream surfaces that replace the blades themselves. To account for profile losses, another force field, $\mathbf{F}_f$, is introduced into the momentum equations to produce entropy, according to the distributed loss model, as proposed in [17]. Moreover, additional terms that consider the blockage due to the tangential blade thickness are introduced into the throughflow model.

The inverse problem consists of finding the unknown stator and rotor camber surfaces $\theta = f(x, r)$ once the tangential component $F_{b\theta}(x, r)$ of the blade force $\mathbf{F}_b$ is prescribed as the design data along the axial and radial directions. These surfaces are considered as deformable and impermeable. They have to be stream surfaces of the absolute/relative motion pertinent to the stator/rotor and have to be orthogonal to the blade force. An initial geometry and flow configuration are guessed as starting conditions of a transient. During the transient, the deformable surfaces move according to the impermeability condition and the prescribed blade loading. As the steady state is reached, the camber surfaces assume the shape that solves the inverse problem.

A. Governing Equations

Let us take into consideration the unsteady motion of an inviscid compressible fluid. The governing Euler equations are written in the meridional plane with the axisymmetric approximation. In a cylindrical frame of reference, the system of equations with volume forces acting on the fluid, in divergence form, reads as

$$\nabla \cdot [\mathbf{V}] = \boldsymbol{Q} - (1/\boldsymbol{r})\boldsymbol{N} \tag{1}$$

with ∇ and $[\mathbf{V}]$ being, respectively, $\nabla = \frac{\partial}{\partial t}\mathbf{k} + \frac{\partial}{\partial x}\mathbf{i} + \frac{\partial}{\partial r}\mathbf{j}$ and $[\mathbf{V}] = U\mathbf{k} + F\mathbf{i} + G\mathbf{j}$, where $\mathbf{k}$, $\mathbf{i}$, and $\mathbf{j}$ are the unit vectors of a cylindrical frame of reference of the time-space (t, x, r) domain, and

$$U = \begin{Bmatrix} \rho \\ \rho u \\ \rho v \\ \rho w \\ \rho E \end{Bmatrix} \quad F = \begin{Bmatrix} \rho u \\ \rho u^2 + p \\ \rho uv \\ \rho uw \\ \rho Hu \end{Bmatrix} \quad G = \begin{Bmatrix} \rho w \\ \rho uw \\ \rho vw \\ \rho w^2 + p \\ \rho Hw \end{Bmatrix}$$

$$N = \begin{Bmatrix} \rho w \\ \rho uw \\ 2\rho vw \\ \rho(v^2 - w^2) \\ \rho Hw \end{Bmatrix} \quad Q = \begin{Bmatrix} -b\rho u \\ F_{bx} + F_{fx} - b\rho u^2 \\ F_{b\theta} + F_{f\theta} - b\rho uv \\ F_{br} + F_{fr} - b\rho uw \\ \mathbf{F}_b \cdot \mathbf{q} - b\rho Hu \end{Bmatrix} \tag{2}$$

According to the Gaussian formula, the integral of Eq. (1) in a given volume D of the time-space domain can be written as

$$\int_{\partial D} [\mathbf{V}] \cdot \mathbf{n}\, d\sigma = \int_D Q\, d\tau - \int_D \frac{N}{r}\, d\tau \tag{3}$$

with ∂D being the boundary of the volume D and $\mathbf{n}$ the outward normal.

All the flow properties are normalized with respect to suitable reference values. The blockage effect of the blades is introduced through the factor b, which is given by

$$b = (1/h)(\partial h/\partial x) \tag{4}$$

where h is the free passage that is given, for the axisymmetric problem, by

$$h = 1 - \frac{n\delta(x, r)}{2\pi r} \tag{5}$$

where n is the number of blades.

The stream surfaces that replace the stator and rotor blades are expressed as a function $\theta = f(x, r, t)$ and are treated as additional unknowns. These surfaces change shape during the transient described by Eq. (3) and satisfy the impermeability condition. If the equation of a blade surface is written as

$$\Theta(x, r, \theta, t) = \theta - f(x, r, t) = 0 \tag{6}$$

the impermeability condition is satisfied by imposing, during the transient, the total derivative of the function $\Theta(x, r, \theta, t)$ equal to zero:

$$\frac{D\Theta}{Dt} = \frac{\partial \Theta}{\partial t} + (\mathbf{q} - \boldsymbol{\Omega} \times \mathbf{r}) \cdot \text{grad}\Theta = 0 \tag{7}$$

which, according to Eq. (6), becomes

$$\frac{\partial f}{\partial t} + u\frac{\partial f}{\partial x} + w\frac{\partial f}{\partial r} = \frac{v}{r} - \Omega \tag{8}$$

where Ω is the angular velocity of the rotor, which is always equal to zero for stator blades. The other two components of the blade forces, F_{bx} and F_{br}, which appear in Eq. (2), are related to the tangential component $F_{b\theta}$ by the orthogonality conditions, given by

$$F_{bx} = -r\frac{\partial f}{\partial x}F_{b\theta} \qquad F_{br} = -r\frac{\partial f}{\partial r}F_{b\theta} \tag{9}$$

The external friction force introduced by the distributed loss model replaces the viscous terms, produces entropy, and acts in the opposite direction to the flow velocity vector. The second law of thermodynamics then gives [17]

$$\rho T\frac{Ds}{Dt} = \rho T\left(\frac{\partial s}{\partial t} + u\frac{\partial s}{\partial x} + w\frac{\partial s}{\partial r}\right) = -\mathbf{q} \cdot \mathbf{F}_f \tag{10}$$

B. Numerical Method

The system of Eqs. (1–3) is approximated using a finite volume technique by discretizing the (x, r) plane by means of four-sided cells whose shape does not depend on time. An upwind finite volume method, inspired by Godunov's flux difference splitting idea [18], is used. A two-step, predictor-corrector integration scheme that belongs to the second-order class according to the essentially nonoscillatory (ENO) concept [19] is adopted. The resulting scheme is second-order accurate in both time and space. Three boundary conditions have to be imposed at the inlet if the flow is subsonic: total pressure, total temperature, and flow angles. All the flow properties have to be given for a supersonic inlet. No boundary conditions are needed at the exit if the flow is supersonic, whereas for the subsonic case one boundary condition must be prescribed, which is, as usual, the static pressure distribution. As stressed in [8], in the formulated inverse method, this choice does not in fact produce a stable solution when high flow deflections are searched for. To be able to compute the camber geometry of turbine blades, a mass flow is actually prescribed at the exit for a nonchoked flow. Moreover, a nonreflecting boundary condition is imposed, according to [20], to eliminate incoming waves. One condition is needed at impermeable boundaries. This condition is prompted by the physics of the problem: at solid annulus walls, the vanishing of the normal velocity component is imposed, whereas at flexible walls, that is, in the regions containing the blade rows, the volume force $F_{b\theta}$ is prescribed as the design data, according to the inverse problem formulation.

Once the fluid dynamics problem is solved, the wall geometry is updated at each time step by enforcing the impermeability conditions. Each point of the stream surface has to move with a normal velocity equal to the normal component of the flow velocity during the transient. This is accomplished by integrating Eq. (8) in time. The space derivatives of $f(x, r, t)$ are then computed and the other two components of the blade force, F_{bx} and F_{br}, are evaluated from relations (9).

As an example, the time evolution of the flexible surface evaluated by the inverse method is shown in Fig. 1. A two-dimensional stator blade is considered and is positioned between $x = 0.0$ and 1.0. In the example, the prescribed blade loading has been assumed constant along the span, whereas along the x axis it has the prescribed distribution shown in the lower part of Fig. 1. A plane surface has been assumed as a starting geometry of the camber and its trace in the tangential plane, labeled $k = 0$, is shown in Fig. 1. The initial profile, which is quite far from the final one, evolves during the transient and the shapes assumed at different time steps, K, are plotted in the same picture. At the time step $K = 10,000$, the flow field has reached a steady state and, as a consequence, the surface assumes a shape that remains unchanged $(k = 13,000)$ and satisfies the prescribed loading distribution.

The proposed inverse technique has been validated extensively in works previously carried out on the matter, as reported in [6–8,21]. Analytical, numerical, and experimental comparisons have been performed for channel and blade rows, including transonic flow configurations. Among them, it is worth mentioning the check against the analytically known Ringleb flow. In this test case, two streamlines of the flow were considered as the unknown walls of a channel that had to be evaluated using the inverse problem for which the theoretical pressure distributions along the walls themselves were prescribed as the design data. The flowfield and wall geometries computed by the inverse method were shown to be in agreement with the theoretical ones.

In the aforementioned references, the solution uniqueness of the inverse design for the blade row was also considered. Briefly, for the sake of simplicity, let us consider a steady-state flow through a two-dimensional cascade. As is well known, the tangential

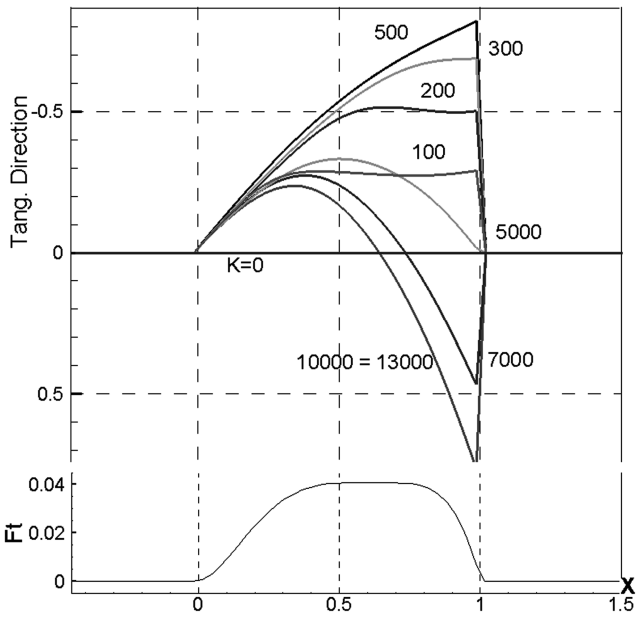

Fig. 1 Time evolution of the camber surface and loading distribution along x.

component of the force acting on the blade is related to the mass flow and to the far upstream and downstream tangential components of the flow velocity. The same total force on the blade can be accomplished with two possible physical configurations: one has a large mass flow and a small flow deflection, whereas the other has a smaller mass flow and a larger deflection. When the inverse problem is solved by imposing the proper boundary conditions and a prescribed loading distribution on the blade, the following situations can occur: 1) if the integral along the axial direction of the loading is greater than a maximum value, or smaller than another value, the procedure will not be able to find any solution, as expected; otherwise, 2) if the pressure is imposed as the exit boundary condition, the calculation converges to the solution with the smaller deflection and the larger mass flow, whereas the numerical procedure is not able to reach a stable solution for the other configuration, even though it is stable from a physical point of view; and c) if a mass flow is prescribed at the exit, the computation can even obtain a stable solution for the configuration with the larger deflection.

C. Optimization Procedure

A multi-objective genetic algorithm has been implemented in the proposed optimization procedure. It involves the classical genetic operators: real valued and binary-coded design variables; a tournament selection scheme; a simulated binary crossover and one point-crossover for real- and binary-coded variables, respectively; and a mutation operator. The algorithm is based on a search for nondominated solutions, that is, the Pareto-optimal set. The nondominated sorting GA approach and an efficient constraint handling technique, which avoid the introduction of any penalty parameter, are used to rank each solution in the population, as proposed in [22]. The procedure for the reproduction operator, applied to a population, is based on a tournament scheme in which individuals are randomly chosen and compete on the basis of the following rules: 1) among all individuals that represent feasible solutions, the best ranked element wins; 2) any feasible solution is preferred to any infeasible one; and 3) among infeasible solutions, the individual with the smallest constraint violation is chosen.

As a result, in the constrained-domination approach, any feasible solution has a better nondomination rank than any infeasible solution. Moreover, the multi-objective algorithm is conceived to ensure elitism and to preserve diversity among the solutions of the Pareto-optimal front [23].

III. Three-Dimensional Aspects

The fully three-dimensional flows caused by annulus walls, by the change of the blade shape in the spanwise direction, by a staking line geometry, and by inlet flow distortions cannot be predicted using a throughflow model. Nevertheless, some of these aspects can be introduced in the early stage of the turbomachine design, even with the simplified model that has been adopted. Secondary flows and axial velocity profiles can in fact be controlled, to a certain extent, by the lean and sweep of the blades and, in turn, by the suitable stream-surface geometry that is considered in the present throughflow model. The matter was investigated and discussed in the pioneering works of Smith and Yeh [24] and Csanady [25]. The effect of the lean and sweep can be connected to the field force which, in the axisymmetric flow model, replaces the stator and rotor blade rows. Let us consider the steady-state equation of the motion in Crocco's form, which, in an absolute frame of reference, is given by

$$-\mathbf{q}\times\boldsymbol{\omega} = T\,\mathrm{grad}\,s - \mathrm{grad}\,H + (\mathbf{F}_b/\rho) \tag{11}$$

At the steady state, the force $\mathbf{F}_b$ is orthogonal to both $\mathbf{q}$ and $\boldsymbol{\omega}$, when homoentropic and homoenergetic flow is considered (in a relative frame, the total rothalpy and relative vector velocity replace H and $\mathbf{q}$, respectively). From Eq. (11), when the blade force $\mathbf{F}_b$ has only tangential and axial components that do not change in the spanwise direction, the vorticity vector $\boldsymbol{\omega}$ is purely radial. When the blade is swept and/or leaned, all three components of the blade force vary along the blade. As a consequence, the vorticity $\boldsymbol{\omega}$ has an axial component that is responsible for the development of a secondary flow in a plane normal to the machine axis. It is also evident from Eq. (11) that a distortion of the inlet flow, in terms of entropy and/or total enthalpy, and a nonuniform rotor work distribution along the span influence the vorticity components.

According to these considerations, a control of these effects can be attempted and exerted through an appropriate distribution of $\mathbf{F}_b$ in the design process. In the inverse approach considered here, this can be accomplished using the optimization procedure in which the design parameters, that is, the F_θ distribution along the blade, define the search space for suitable objectives. Moreover, this approach makes it possible to investigate the influence of some geometrical parameters, such as the lean and/or sweep of the stream surfaces, on the axial and radial components of $\mathbf{F}_b$ and, in turn, on $\boldsymbol{\omega}$.

IV. Numerical Examples

Some numerical tests are presented in this section. They were conceived to study the effectiveness of the proposed optimization procedure and, as such, they have a preliminary nature. The first one refers to the inverse problem of a linear cascade, whereas the second one shows the design of a single-stage compressor. In all the examples, the friction force $\mathbf{F}_f$ in Eqs. (1–3) is not considered because 1) the rotational flow aspects can be described on a purely inviscid Euler flow basis, and 2) efficiency related to the blade friction forces is not investigated here.

The influence of $\mathbf{F}_f$ on the blade geometry and on the efficiency is discussed in [26].

To have a limited number of design variables, a parameterization is introduced: the blade loading distribution is expressed by means of a parametric surface, instead of a large number of points related to the grid. The $F_{b\theta}(x, r)$ of each blade is defined using Bezier surfaces of order 5×4. The control points are defined so that $F_{b\theta}(x^{\mathrm{LE}}, r) = 0.0$ and $F_{b\theta}(x^{\mathrm{TE}}, r) = 0.0$ along the leading (LE) and trailing edges (TE) of each blade.

The lean and sweep of the blades are also modeled using parametric curves. The leading-edge geometry in the (r, θ) plane defines the blade lean and is described by a Bezier curve of order 3. The first control point is fixed to the hub, whereas the last control point can move along the tip, where r is given. The sweep is defined through the LE and TE geometries in the meridional plane (x, r), which are parameterized by two Bezier curves of the third order. The first control point for each curve is given by the LE and the TE coordinates at the hub, respectively. The last control points of the curves can move in an axial direction along the prescribed annulus contour.

A. Linear Cascade

In the first example, that is, the linear cascade, the inverse problem is solved on a two-dimensional Cartesian frame of references; therefore, the source term N disappears in Eqs. (1–3), and the free passage h introduced in Eq. (4), the impermeability condition, Eq. (8), and the blade force components, Eq. (9), become, respectively

$$h = 1 - \frac{\delta(x, r)}{d} \qquad \frac{\partial f}{\partial t} + u\frac{\partial f}{\partial x} + w\frac{\partial f}{\partial r} = v$$

$$F_{bx} = -\frac{\partial f}{\partial x}F_{b\theta} \qquad F_{br} = -\frac{\partial f}{\partial r}F_{b\theta}$$

where r indicates the Cartesian ordinate.

The tangential blade force is defined along the x direction through a prescribed distribution law, and it is kept constant along the span. The overall blade loading, expressed as the integral of $F_{b\theta}$ on the projection B of the blade stream surface on the (x, r) plane,

$$\int_B F_{b\theta}\,\mathrm{d}x\,\mathrm{d}r$$

has a prescribed value of 0.2. A total pressure $P^0 = 1.0$, a total temperature $T^0 = 1.0$, and an absolute flow angle equal to 50 deg are prescribed at the inlet; $\rho u = 0.18$ is given at the exit section. The maximum tangential thickness has been kept constant along the span

and it has been located at 50% of the axial chord. Because the flowfield has $S = \text{const}$, $H = \text{const}$, and F_θ assumes a uniform value along the span, the vorticity vector $\boldsymbol{\omega}$ does not have an axial component, according to Eq. (11). The corresponding blade has to be cylindrical. To test the capability of the method to converge to the right solution, the control, in the optimization procedure used in this test case, is given by the lean and sweep parameters that describe the blade. According to the prescribed loading, the inverse problem is solved in the (x, r) plane discretized by 60×10 grid points. In the optimization process, a stream-surface geometry is searched for by minimizing the streamwise component of the flow vorticity. The functional is defined as

$$F1(U) = \int_B \boldsymbol{\omega} \cdot \mathbf{q}\, \mathrm{d}x\, \mathrm{d}r$$

The procedure converges to the right solution, as shown in Fig. 2. The geometry of the final stream surface with iso-F_θ is reported in Fig. 2a. The blade profile, constructed on the computed camber surface using the given tangential thickness distribution, is also depicted in the picture. The (x, r) plane section is shown in Fig. 2b, in which the isopressure contours are reported. The geometry and flow uniformity in the spanwise direction are evident in these figures.

A distorted flow is now considered at the inlet by introducing a parabolic distribution for P^0 with a unit value at midspan and a 10% defect at the hub and tip, whereas the other boundary conditions are the same as before. The overall blade loading is prescribed and it has the same value as in the previous example. The same blade loading will produce a higher deflection for a reduced total pressure level or, vice versa, the same flow deflection will require a lower blade loading. Again, in the optimization process, the blade mean cumber surface has been searched for, but, in this case, the parameters describing the blade loading $F_\theta(x, r)$ are introduced as design variables. Two objective functions have been introduced: 1) minimize $F1(\mathbf{U})$, defined as the difference between the actual tangential blade loading and the prescribed one; and 2) minimize the streamwise component of flow vorticity,

$$F2(U) = \int_B \boldsymbol{\omega} \cdot \mathbf{q}\, \mathrm{d}x\, \mathrm{d}r$$

The influence of lean is accounted for by considering the pertinent parameters in the optimization process. The proposed GA has been run for 80 individuals and 100 generations. The Pareto-optimal front obtained at the end of the optimization process is presented in Fig. 3 and labeled P1. The conflicting nature of the two objectives is clearly shown by the nondominated solutions. The optimal configurations located at the extreme points of the Pareto front P1, indicated as A and B, are illustrated in Fig. 4. The blade geometry with a prescribed tangential thickness, the isovorticity contours, and the geometry of the camber surfaces of the linear cascade referring to the selected design points have been depicted in the figures. The blade with a higher loading (design A) shows a compound lean, a nonuniform spanwise blade loading, and a concentration of streamwise vorticity in the hub and tip regions. The blades with a lower loading (design B), and therefore a lower deflection, have smaller streamwise vorticity components. From this point of view, the extreme right individuals on front P1 of Fig. 3 have lower practical interest because of the low loading. The search for optimal solutions should be performed in a search space that is narrowed by appropriate constraints acting on the design variables, that is, blade loading, to exploit the left region of P1. Nevertheless, the influence of lean is highlighted in the same figure. Here, a Pareto front (labeled P2),

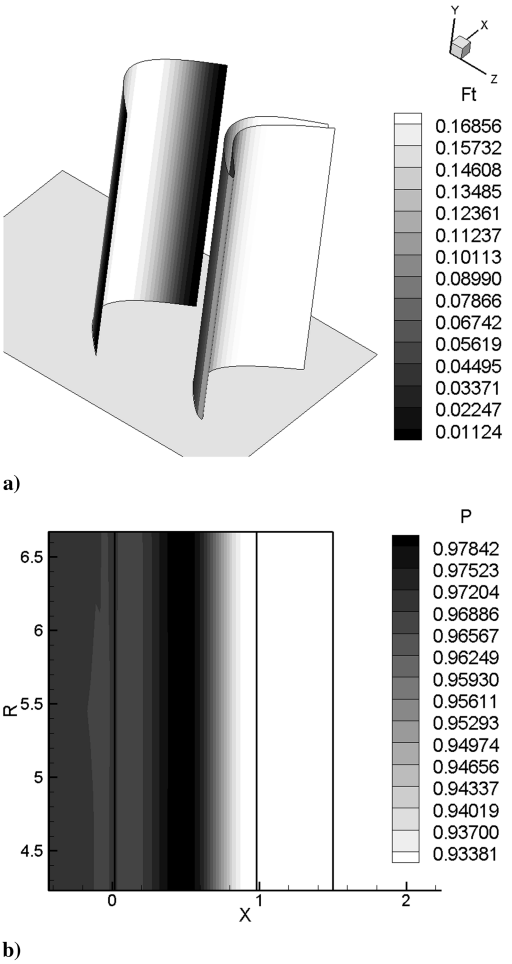

Fig. 2 Linear cascade: a) 3-D camber surface, iso-F_θ, and blade geometry; b) isopressure in the (x, r) plane.

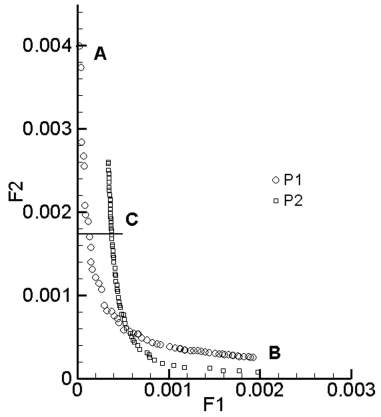

Fig. 3 Pareto fronts in optimization processes for the linear cascade: P1 with lean, P2 without lean.

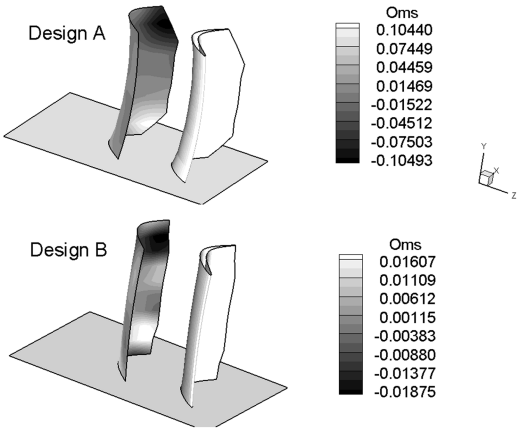

Fig. 4 Cascade design configurations: stream surfaces and iso $(\boldsymbol{\omega} \cdot \mathbf{q})$ vorticity contours on stream surfaces, and blade geometries for designs A and B of the P1 Pareto front.

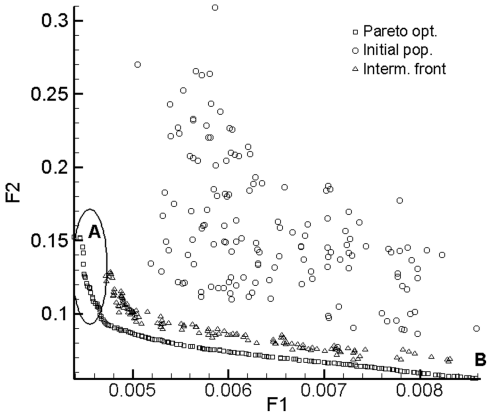

Fig. 5 Compressor stage: initial population, an intermediate nondominated front, and the converged Pareto front.

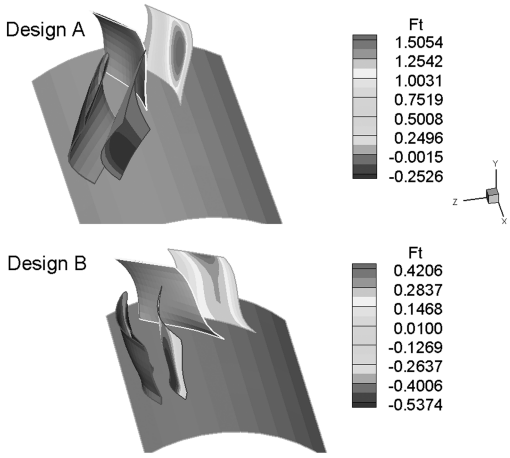

Fig. 6 Compressor stage: iso-$F_{b\theta}$ curves on stream surfaces and geometries for designs A and B.

which refers to another optimization cycle in which the search space is only defined by the tangential force $F_\theta(x, r)$, is also depicted.

It can be seen in Fig. 3 that, if two individuals at the same level of vorticity, that is, $F2$, are considered, a solution (e.g., C in the figure) that belongs to the P2 front, and which therefore describes a blade obtained without a leaning control, has a lower blade loading.

B. Compressor Stage

The last example refers to the design of a single-stage compressor. The design data are given in nondimensional terms as follows: at the inlet, parabolic distribution of the total pressure with $P^0 = 1.0$ at the midspan and with a 10% reduction at the hub and tip regions, total temperature $T^0 = 1.0$, and absolute flow angle equal to 0 deg; a static pressure $p = 0.92$ is imposed at the exit section. The stage total pressure ratio is equal to 1.2, and $\Omega = 0.6$. The work per unit time done by a rotor is expressed as

$$W = \int_B F_\theta \Omega r \, \mathrm{d}x \, \mathrm{d}r$$

where B represents the projection of the rotor stream surface on the meridional plane.

The rotor and stator cambers are evaluated using the inverse problem in which the $F_\theta(x, r)$ distributions on the stator and rotor blades are searched for through the optimization of two functionals defined as follows: 1) minimize the difference between the actual rotor work and the prescribed work W_d, $F1(U) = W - W_d$; and 2) minimize the streamwise component of flow vorticity $F2(U) = \int_B \boldsymbol{\omega} \cdot \mathbf{q} \, \mathrm{d}x \, \mathrm{d}r$.

Design parameters that define the lean and the sweep of the rotor, and the lean of the stator, are also introduced into the process to pursue the stated objectives. Two constraints are also imposed: stator overall loading $\leq$ rotor overall loading, and the continuity of surface slope in a radial direction.

The Pareto-optimal front obtained at the end of the optimization process is presented in Fig. 5. The picture shows the initial population with 150 individuals, an intermediate nondominated front, and the converged Pareto front obtained after 100 generations. Once again, the conflicting nature of the two objectives is evident. The extreme right individuals correspond to not very attractive solutions, because of a low work value of the stage. However, if the solutions in the extreme left region of the Pareto front are considered (the ones in the closed curve of Fig. 5), they represent a design of compressors for which a reduction of 2% of work with respect to the W_d undergoes a reduction of more than 60% of the streamwise vorticity ($F2$).

The optimal configurations located at the extreme points of the Pareto front (designs A and B in Fig. 5) are illustrated in Fig. 6. A rear

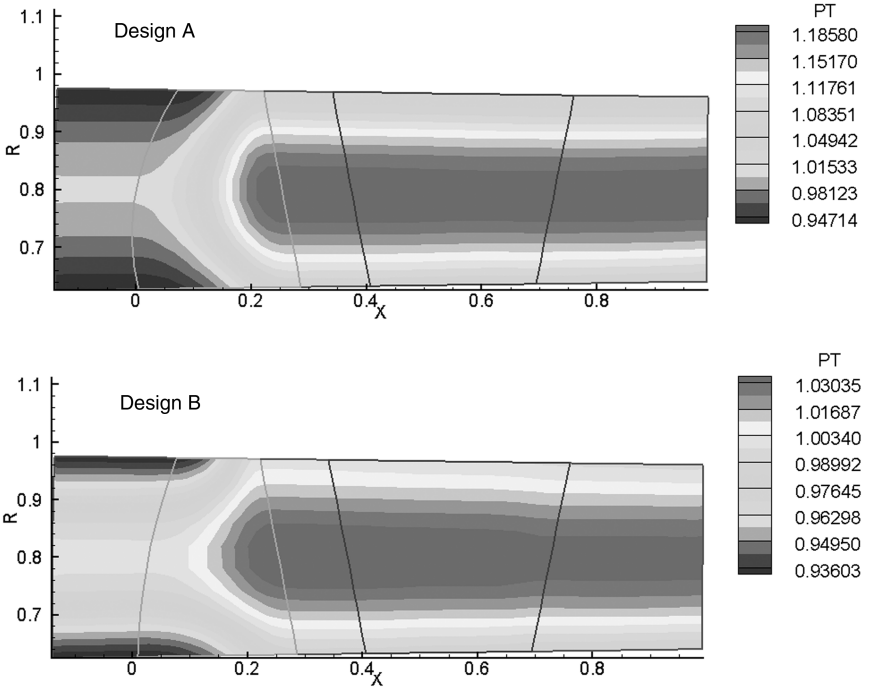

Fig. 7 Compressor stage: isototal pressure contours for designs A and B.

view of the camber surface geometries of the stator and the rotor, and the iso-$F_{b\theta}$ curves referring to the selected points, are drawn in the pictures.

The blades geometries obtained by superimposing the prescribed tangential thickness onto the camber surfaces are also shown here. The first solution, A, maximizes the stage work, whereas the second one, B, minimizes the streamwise vorticity. Even though the effect of lean and/or sweep cannot in general be stated, the influence of these parameters on the radial loading distribution and on the vorticity can be assessed in the optimization procedure, in the limit of validity of the axisymmetric model. Both the rotor and stator present a compound lean and a nonuniform radial $F_{b\theta}$. Because the blade loading assumes a lower value at the hub and tip than at the midspan section, the overall loss generation tends to be reduced. The sweep and lean that give a three-dimensional configuration of blade surfaces and the blade loading distributions are also evident from these figures. Finally, the isototal pressure contours in the meridional plane, for designs A and B, are shown in Fig. 7. The radial distribution reveals that the increment of the total pressure essentially occurs in the core of the rotor blade, where a more efficient transformation is supposed to happen. For both designs A and B, the pressure ratio delivered by the compressor stage is higher at the midspan than at the end walls and the lower levels of total pressure are always confined to the tip and hub regions.

V. Conclusions

An optimization procedure to design stator and rotor blades of axial turbomachines, based on the inverse problem solution, has been developed. It relies on the use of a multi-objective genetic algorithm to search for an optimal distribution of the blade force that is used as the design data in the inverse problem. The solution is represented by the geometry of stream surfaces that substitute the stators and rotors of a three-dimensional axial turbomachine, approximated by a throughflow axisymmetric Euler model. The search space has been extended to also include geometric parameters, such as the blade lean and sweep, and it has been limited by simple geometrical constraints. Some preliminary results show the capability of the approach of taking into account some 3-D effects in the preliminary blade design.

Acknowledgment

This work has partly been funded by the Regione Piemonte, Italy (Bando regionale per la ricerca industriale e lo sviluppo precompetitivo per l'anno 2006).

References

[1] Lapworth, B. L., and Shahpar, S., "Design of Gas Turbine Engines Using CFD," *ECCOMAS 2004 Proceedings*, European Congress on Computational Methods in Applied Sciences and Engineering, Barcelona, July 2004, pp. 1–21.

[2] Denton, J. D., and Dawes, W. N., "Computational Fluid Dynamics for Turbomachinery Design," *Proceedings of the Institution of Mechanical Engineers, Part C: Journal of Mechanical Engineering Science*, Vol. 213, No. 2, 1998, pp. 107–124. doi:10.1243/0954406991522211

[3] Sturmayr, A., and Hirsch, C., "Throughflow Model for Design and Analysis Integrated in a Three-Dimensional Navier-Stokes Solver," *Institution of Mechanical Engineers Part A: Journal of Power and Energy*, Vol. 213, No. 4, 1999, pp. 263–273. doi:10.1243/0957650991537608

[4] Simon, J., and Léonard, O., "Modeling of 3-D Losses and Deviations in a Throughflow Analysis Tool," *Journal of Thermal Science*, Vol. 16, No. 3, 2007, pp. 208–214. doi:10.1007/s11630-007-0208-x

[5] Bena, C., Larocca, F., and Zannetti, L., "Design of Multi-Stage Axial Flow Turbines and Compressors," *3rd European Conference on Turbomachinery*, Institution of Mechanical Engineers, London, 1999, pp. 635–644.

[6] Zannetti, L., "Time Dependent Method to Solve Inverse Problems for Internal Flows," *AIAA Journal*, Vol. 18, No. 7, 1980, pp. 754–758. doi:10.2514/3.50816

[7] Ferlauto, M., Larocca, F., and Zannetti, L., "Integrated Design and Analysis of Intakes and Nozzles in Air-Breathing Engines," *Journal of Propulsion and Power*, Vol. 18, No. 1, 2002, pp. 28–34.

[8] Zannetti, L., and Larocca, F., "Inverse Methods for 3D Internal Flows," AGARD Rept. 780, May 1990.

[9] Dang, T., Damle, S., and Qiu, X., "Euler-Based Inverse Method for Turbomachine Blades, Part 2: Three Dimensions," *AIAA Journal*, Vol. 38, No. 11, 2000, pp. 2007–2013.

[10] Dennis, B. H., Dulikravich, G. S., and Han, Z.-X., "Constrained Optimization of Turbomachinery Airfoil Shapes Using a Navier-Stokes Solver and a Genetic/SQP Algorithm," *Journal of Propulsion and Power*, Vol. 17, No. 5, 2001, pp. 1123–1128.

[11] Dulikravich, G. S., Martin, T. J., Dennis, B. H., and Egorov, I. N., "Aero-Thermal-Elasticity-Materials Optimization of Cooled Gas Turbine Blades: Parts 1–2," *Lecture Series on Numerical Optimization Methods & Tools for Multi-Criteria/Multi-Disciplinary Design with Applications to Aeronautics and Turbomachinery*, Von Karman Institute for Fluid Dynamics, Belgium, Nov. 2004.

[12] Pierret, S., Coelho, F. R., and Kato, H., "Multidisciplinary and Multiple Operating Points Shape Optimization of Three-Dimensional Compressor Blades," *Structural and Multidisciplinary Optimization*, Vol. 33, No. 1, 2006, pp. 61–70. doi:10.1007/s00158-006-0033-y

[13] Karakasis, M. K., and Désidéri, J.-A., "Model Reduction and Adaption of Optimum-Shape Design in Aerodynamics by Neural Networks," French National Institute for Research in Computer Science And Control Rept. 4503, 2002.

[14] Pierret, S., and Van den Braembussche, R. A., "Turbomachinery Blade Design Using a Navier-Stokes Solver and Artificial Neural Network," *Journal of Turbomachinery*, Vol. 121, No. 2, 1999, pp. 326–332.

[15] Kelner, V., Grondin, G., Leonard, O., and Moreau, S., "Multi-Objective Optimization of a Fan Blade by Coupling a Genetic Algorithm and a Parametric Flow Solver," *Proceedings of the 6th International Conference on Evolutionary Computing for Industrial Application* , edited by R. Schilling, W. Haase, J. Periaux, H. Baier, and G. BugedaMunich, FLM, Munich, Sept. 2005, pp. 1–12.

[16] Petrovic, M. V., Dulikravich, G. S., and Martin, T. J., "Optimization of Multistage Turbines Using a Through-Flow Code," *Journal of Power and Energy*, Vol. 215, No. 5, 2001, pp. 559–569. doi:10.1243/0957650011538802

[17] Hirsch, C., *Numerical Computation of Internal and External Flows Vol. 1: Fundamentals of Numerical Discretization*, Wiley, Chichester, England, U.K., 1988, Chap. 2.

[18] Osher, S., and Solomon F., "Upwind Difference Schemes for Hyperbolic System of Conservative Laws," *Mathematics of Computation*, Vol. 38, No. 158, 1982, pp. 339–374. doi:10.2307/2007275

[19] Harten, A., Engquist, B., and Osher, S., "Uniformly High Order Accuracy Essentially Non-Oscillatory Schemes, III," *Journal of Computational Physics*, Vol. 71, No. 2, 1987, pp. 231–303. doi:10.1016/0021-9991(87)90031-3

[20] Rudy, D., and Strikwerda, J. A., "Non-Reflecting Outflow Boundary Condition for Subsonic Navier-Stokes Calculations," *Journal of Computational Physics*, Vol. 36, No. 1, 1980, pp. 55–70. doi:10.1016/0021-9991(80)90174-6

[21] Larocca, F., and Zannetti, L., "Design Methods for Two-Dimensional Transonic Rotational Flows," AIAA Paper 95-0648, Jan. 1995.

[22] Deb, K., Pratap A., Agarwal, S., and Meyarivan, T., "A Fast and Elitist Multi-Objective Genetic Algorithm: NSGA-II," *IEEE Transactions on Evolutionary Computation*, Vol. 6, No. 2, 2002, pp. 182–197. doi:10.1109/4235.996017

[23] Deb, K., Mohan, M., and Mishra, S., "Towards a Quick Computation of Well-Spread Pareto-Optimal Solutions," *Evolutionary Multi-Criterion Optimization*, Lecture Notes in Computer Science, Vol. 2632, Springer–Verlag, Berlin/Heidelberg, 2003, pp. 222–236.

[24] Smith, L. H., and Yeh, H., "Sweep and Dihedral Effect in Axial Flow Turbomachinery," *Journal of Basic Engineering*, Vol. 85, No. 3, 1963, pp. 401–416.

[25] Csanady, G. T., "Discussion on the Paper by Smith and Yeh," *Journal of Basic Engineering*, Vol. 85, No. 3, 1963, pp. 414–415.

[26] Rosa Taddei S., and Larocca, F., "Axisymmetric Design of Axial Turbomachines: An Inverse Method Introducing Profile Losses," *Proceedings of the Institution of Mechanical Engineers. Part A, Journal of Power and Energy* (to be published).

A. Prasad
Associate Editor